ARTICLE

Mutations within the selectivity filter reveal that Kv1 channels have distinct propensities to slow inactivate

Xiaosa Wu[1], Kanchan Gupta[1], and Kenton J. Swartz[1]

Voltage-activated potassium (Kv) channels open in response to membrane depolarization and subsequently inactivate through distinct mechanisms. For the model Shaker Kv channel from *Drosophila*, fast N-type inactivation is thought to occur by a mechanism involving blockade of the internal pore by the N-terminus, whereas slow C-type inactivation results from conformational changes in the ion selectivity filter in the external pore. Kv channel inactivation plays critical roles in shaping the action potential and regulating firing frequency, and has been implicated in a range of diseases including episodic ataxia and arrhythmias. Although structures of the closely related Shaker and Kv1.2 channels containing mutations that promote slow inactivation both support a mechanism involving dilation of the outer selectivity filter, mutations in the outer pores of these two Kv channels have been reported to have markedly distinct effects on slow inactivation, raising questions about the extent to which slow inactivation is related in both channels. In this study, we characterized the influence of a series of mutations within the external pore of Shaker and Kv1.2 channels and observed many distinct mutant phenotypes. We find that mutations at four positions near the selectivity filter promote inactivation less dramatically in Kv1.2 when compared to Shaker, and they identify one key variable position (T449 in Shaker and V381 in Kv1.2) underlying the different phenotypes in the two channels. Collectively, our results suggest that Kv1.2 is less prone to inactivate compared to Shaker, yet support a common mechanism of inactivation in the two channels.

Introduction

Voltage-activated potassium (Kv) channels are a large and diverse family of membrane proteins that open in response to membrane depolarization to provide a pathway for K^+ ions to diffuse across the membrane to repolarize membrane voltage (Yellen, 2002). They are widely expressed in neurons, cardiac and skeletal muscle cells, as well as in many other cell types within the body, playing many key roles in human physiology (Yellen, 2002; Wulff et al., 2009; Jan and Jan, 2012). Perturbations in the functional properties of many Kv channels are implicated in a range of diseases, including cardiac arrhythmias, episodic ataxia, and epilepsy (Adelman et al., 1995; Hubner and Jentsch, 2002; Yellen, 2002; Kurata and Fedida, 2006; Wulff et al., 2009; Jan and Jan, 2012).

The Shaker Kv channel from *Drosophila melanogaster* was the first Kv channel to be cloned (Papazian et al., 1988), and it has served as a model for understanding key functional mechanisms. Similarly, the mammalian Kv1.2 relative of Shaker has

provided a structural foundation for understanding Kv channel mechanisms (Long et al., 2005a, Long et al., 2005b), with the X-ray structure of the Kv1.2/2.1 paddle chimera serving as a widely used structural model for many Kv channels (Alabi et al., 2007; Long et al., 2007). Both functional and structural studies have shown that Kv channels are tetramers (MacKinnon, 1991; Doyle et al., 1998; Long et al., 2005a), with each subunit containing six transmembrane segments, termed S1–S6 (Fig. 1 B). A central pore domain is formed by the tetrameric arrangement of the S5–S6 segments, with the external pore containing the selectivity filter (SF; Fig. 1 B) responsible for the exquisite selectivity of these channels for K^+ ions (MacKinnon and Yellen, 1990; Heginbotham et al., 1994). On the intracellular end of the pore, the four S6 segments form an intracellular activation gate that prevents the flow of ions in the closed state (Holmgren et al., 1997; Liu et al., 1997; Holmgren et al., 1998; del Camino et al., 2000; del Camino and Yellen, 2001). The S1–S4 segments

[1]Molecular Physiology and Biophysics Section, Porter Neuroscience Research Center, National Institute of Neurological Disorders and Stroke, National Institutes of Health, Bethesda, MD.

Correspondence to Kenton J. Swartz: Kenton.Swartz@nih.gov

Kanchan Gupta's present address is Rubius Therapeutics, Cambridge, MA.

from each subunit form peripheral voltage-sensing domains that activate in response to membrane depolarization to open the intracellular activation gate and support ion permeation (Bezanilla, 2008; Swartz, 2008; Bezanilla, 2018).

Ion permeation through the Shaker Kv channel can be diminished in response to sustained depolarization by two forms of inactivation that have distinct mechanisms and timescales (Hoshi et al., 1990; Zagotta et al., 1990; Hoshi et al., 1991; Lopez-Barneo et al., 1993). N-type inactivation in the Shaker channel develops on the millisecond timescale and is thought to involve blockade of the internal pore by a peptide located at the N-terminus (Hoshi et al., 1990; Zagotta et al., 1990) or provided by auxiliary β-subunits in the case of mammalian Kv1 relatives of Shaker (Rettig et al., 1994). In contrast, C-type inactivation develops more slowly and involves conformational changes in the SF within the external pore that is sensitive to the concentration of external K⁺ ions, blockers like tetraethylammonium or mutations near the SF (Choi et al., 1991; Hoshi et al., 1991; Lopez-Barneo et al., 1993; Perozo et al., 1993; Yellen et al., 1994; Baukrowitz and Yellen, 1995; Liu et al., 1996; Molina et al., 1997; Starkus et al., 1997; Yang et al., 1997; Ogielska and Aldrich, 1998; Ogielska and Aldrich, 1999; Yang et al., 2002; Kitaguchi et al., 2004; Kurata and Fedida, 2006; Hoshi and Armstrong, 2013; Pless et al., 2013). The T449 position near the SF in Shaker is a particularly critical position where hydrophobic or polar substitutions dramatically slow or speed C-type inactivation, respectively (Lopez-Barneo et al., 1993; Molina et al., 1997; Yang et al., 2002; Kitaguchi et al., 2004).

Recent structures of mutant Shaker and Kv1.2 channels suggest that C-type inactivation results from a dilation in the external half of the SF, disrupting two of the four K⁺ ion binding sites that are essential for ion permeation (Fig. 1, C and D; Reddi et al., 2022; Tan et al., 2022). In the case of Shaker, dilation of the SF was observed in the W434F mutant (Fig. 1, D–F) that so strongly promoted C-type inactivation that the channel was effectively non-conducting (Yang et al., 1997). A similar phenotype is also seen in the D447N mutation (Hurst et al., 1996; Pless et al., 2013), and in most K⁺ channel structures the residues equivalent to W434 and D447 in Shaker form a hydrogen bond (Fig. 1 E) to stabilize a conducting state of the SF (Doyle et al., 1998; Long et al., 2005a; Long et al., 2007; Pless et al., 2013). In contrast, the W366F mutation in Kv1.2 (equivalent to W434F in Shaker) speeds inactivation much less dramatically compared to Shaker and remains competent to conduct ions (Suarez-Delgado et al., 2020). Importantly, combining the W366F mutation in Kv1.2 along with V381T, the equivalent of T449 in Shaker, renders the channel non-conducting (Suarez-Delgado et al., 2020), similar to W434F in Shaker. In the case of Kv1.2, dilation of the SF in the C-type inactivated state (Fig. 1, G and H) was observed when combining the equivalent of W366F and V381T along with a third mutation in the Kv1.2/2.1 paddle chimera that improved protein expression (Reddi et al., 2022). Thus, both the Shaker and Kv1.2 structures that point to dilation of the SF during inactivation contain critical mutations, some of which have distinct phenotypes in the two channels, raising questions about the extent to which slow C-type inactivation is related between Shaker and Kv1.2. In addition, although the structural changes

observed in Shaker and Kv1.2 are similar, there are notable differences in the P-loop external to the SF (Reddi et al., 2022). Given the significance of this new mechanism of inactivation, we thought it would be valuable to systematically characterize the functional effects of mutations near the SF in Kv1.2 corresponding to key positions previously studied in Shaker and shown to have pronounced effects on slow C-type inactivation. We systematically compared the influence of inactivation-promoting mutations in Shaker and Kv1.2 channels to understand whether the same network of interacting residues is involved in maintaining a conducting state and to further explore whether the mechanism of slow C-type inactivation is similar in the two channels. Our results identify one critical residue difference between Shaker and Kv1.2 that is largely responsible for the distinct mutant phenotypes we observed in the two channels, and they suggest that Kv1.2 is inherently less prone to inactivate compared to Shaker. Although we observed many distinct mutant phenotypes in Shaker and Kv1.2 channels, our results are consistent with similar mechanisms of C-type inactivation in the two channels.

Materials and methods

Expression of constructs and molecular biology
The rat Kv1.2 channel cDNA in pMAX was kindly provided by Dr. León D. Islas (Universidad Nacional Autónoma de México, Mexico City, Mexico). The Kv1.2/2.1 chimera and Shaker constructs were subcloned into the pGEM-HE vector (Liman et al., 1992) for expression in oocytes. Mutagenesis was performed by Quickchange Lightning Kit (Agilent), and the DNA sequence of all constructs and mutants was confirmed by automated DNA sequencing. cRNA was synthesized using the T7 polymerase (mMessage mMachine kit, Ambion) after linearizing the DNA with appropriate restriction enzymes.

Electrophysiological recordings
All channel constructs were expressed in *Xenopus laevis* oocytes and studied using the two-electrode voltage-clamp technique following 1–6 d of incubation after cRNA injection. The animal care and experimental procedures were performed in accordance with the Guide for the Care and Use of Laboratory Animals and were approved by the Animal Care and Use Committee of the National Institute of Neurological Disorders and Stroke (animal protocol number 1253–17). Oocytes were removed surgically and incubated with agitation for 1 h in a solution containing (in mM) 82.5 NaCl, 2.5 KCl, 1 MgCl₂, 5 HEPES, pH 7.6 (with NaOH), and collagenase (2 mg/ml; Worthington Biochemical). Defolliculated oocytes were injected with cRNA for each of the constructs and incubated at 17°C in a solution containing (in mM) 96 NaCl, 2 KCl, 1 MgCl₂, 1.8 CaCl₂, 5 HEPES, pH 7.6 (with NaOH), and gentamicin (50 mg/ml, GIBCO-BRL). Oocyte membrane voltage was controlled using an OC-725C oocyte clamp (Warner Instruments). Data were filtered at 1 kHz and digitized at 5–10 kHz using pClamp software (Molecular Devices) and a Digidata 1440A digitizer (Axon Instruments). Microelectrode resistances were 0.1–0.5 MΩ when filled with 3 M KCl. The external recording solution contained (in mM) 50 KCl, 50 NaCl, 1 MgCl₂, 0.3 CaCl₂, and 10 HEPES, pH 7.6 (with NaOH).
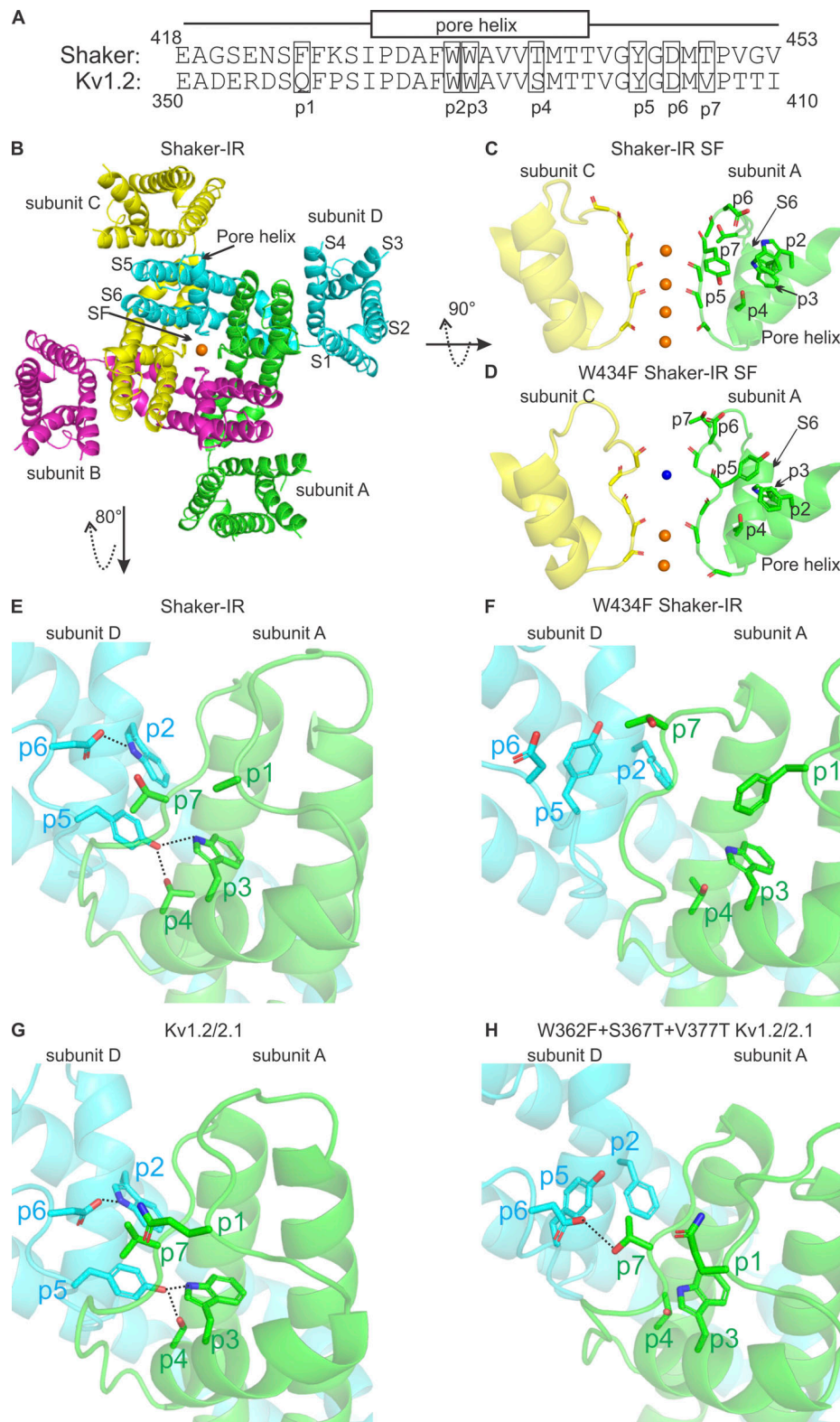
Figure 1. Sequence alignment of Shaker and Kv1.2 channels and structures of the Shaker Kv channel and Kv1.2/2.1 paddle chimera. (A) Sequence alignment of Shaker and Kv1.2 near the SF in the outer region of the pore. p1–p7 are residues where mutations were investigated in this study. **(B)** Extracellular view of the overall structure of Shaker–IR (PDB accession no. 7SIP). **(C)** Structure of the SF of Shaker-IR (PDB accession no. 7SIP); orange spheres represent potassium ions. **(D)** Structure of the SF of Shaker W434F (PDB accession no. 7SJ1); blue sphere represents a water molecule. **(E)** Interactions of residues at p2–p7 in Shaker-IR; the side-chain of the Phe at p1 was not modeled in the structure. **(F)** Interactions of residues at p2–p7 in Shaker-IR W434F. **(G)** Interactions of residues at p2–p7 in the Kv1.2/2.1 paddle chimera (PDB accession no. 2R9R). **(H)** Interactions of residues at p2–p7 in the Kv1.2/2.1 triple mutant channel (W362F/S367T/V377T; p2/p4/p7; PDB accession no. 7SIT). All hydrogen bonds are displayed as dotted black lines.

Table 1. The amino acids and their numbers at p1–p7 in Shaker, Kv1.2, and Kv1.2/2.1 paddle chimera channels

Position	Shaker	Kv1.2	Kv1.2/2.1
p1	Phe425	Gln357	Gln353
p2	Trp434	Trp366	Trp362
p3	Trp435	Trp367	Trp363
p4	Thr439	Ser371	Ser367
p5	Tyr445	Tyr377	Tyr373
p6	Asp447	Asp379	Asp375
p7	Thr449	Val381	Val377

Experiments were performed at room temperature (∼22°C). In most instances, ionic and gating currents were recorded in response to voltage steps using a p/−4 subtraction protocol to subtract capacitive and leak currents. In cases where long pulses were used to study the kinetics of slow inactivation, p/−4 subtraction was not employed.

Results

The objective of the present study was to investigate the influence of a series of mutations at important conserved positions near the SF of Kv1.2 that have been previously studied in the Shaker Kv channel and shown to dramatically influence C-type inactivation. As we will be referring to these positions routinely in Shaker and Kv1.2, and occasionally in the Kv1.2/2.1 paddle chimera, we designated each position as p1–p7, as shown in the sequence alignment in Fig. 1 A, and labeled in the structures of both Shaker and the Kv1.2/2.1 paddle chimera (Fig. 1, B–G; Table 1; Reddi et al., 2022; Tan et al., 2022). As illustrated in the structure of the SF of Shaker-IR (N-type inactivation removed by deletion of residues 6–46), which is similar to many other K⁺ channels thought to represent a conducting state (Doyle et al., 1998; Zhou et al., 2001; Long et al., 2005a; Long et al., 2007), interactions between these conserved residues are important for stabilizing a conducting conformation of the SF (Fig. 1 E). Trp at p2 (W434) and Asp at p6 (D447) form an intrasubunit hydrogen bond, while Tyr at p5 forms intersubunit hydrogen bonds with Trp at p3 and Thr at p4, and each of these interactions has been functionally implicated in stabilizing a conducting state in Shaker (Pless et al., 2013). The Tyr at p5 would also be expected to form hydrophobic interactions with the Thr at p7, and substitutions with more hydrophobic residues at p7 greatly slow C-type inactivation in Shaker (Lopez-Barneo et al., 1993; Molina et al., 1997; Yang et al., 2002; Kitaguchi et al., 2004). In the structure of Shaker W434F (p2), many of these key conserved residues move relative to one
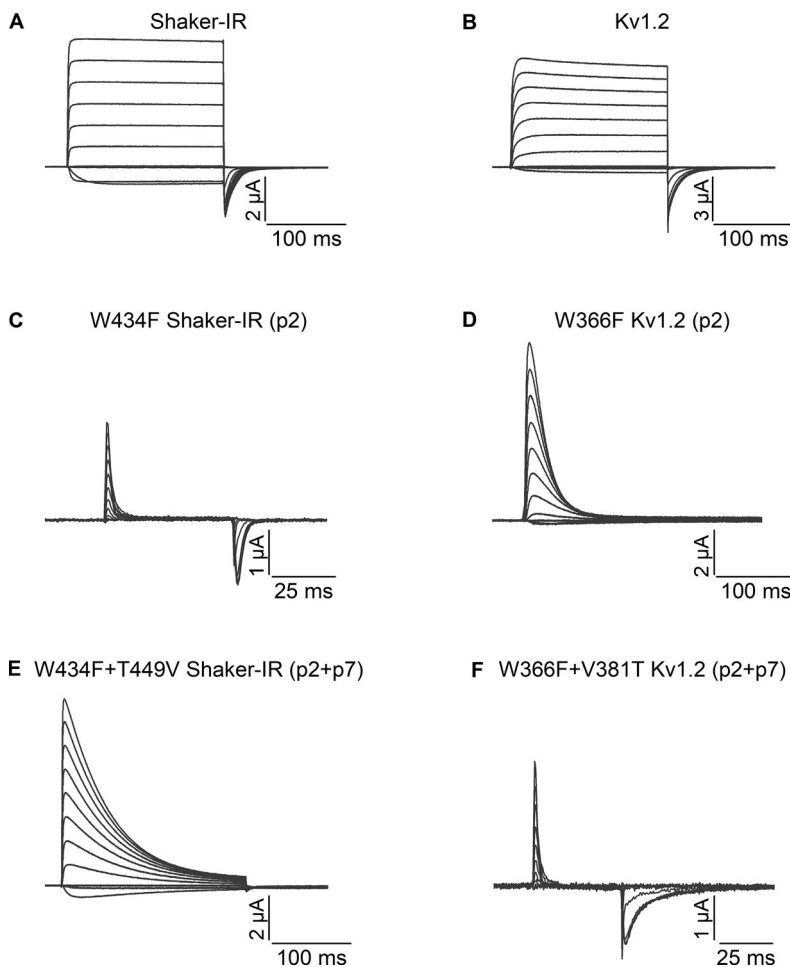

Figure 2. **Ionic and gating current recordings for Shaker and Kv1.2 as well as their mutants at p2 and p7. (A)** Family of ionic currents for Shaker-IR. **(B)** Family of ionic currents for Kv1.2. **(C)** Family of gating currents for Shaker-IR W434F (p2). **(D)** Family of ionic currents for Kv1.2 W366F (p2). **(E)** Family of ionic currents for Shaker-IR W434F/T449V (p2/p7). **(F)** Family of gating currents for Kv1.2 W366F/V381T (p2/p7). For the ionic current recordings, the holding voltage was −90 mV and step depolarizations were from −80 to +50 mV in 10-mV increments, and the tail voltage was −60 mV. For the gating current recordings, the holding voltage was −120 mV, and step depolarizations were from −110 to +20 mV in 10-mV increments to elicit ON gating currents before stepping back to −120 mV to elicit OFF gating currents. These conditions were applied to all other recordings in this study.
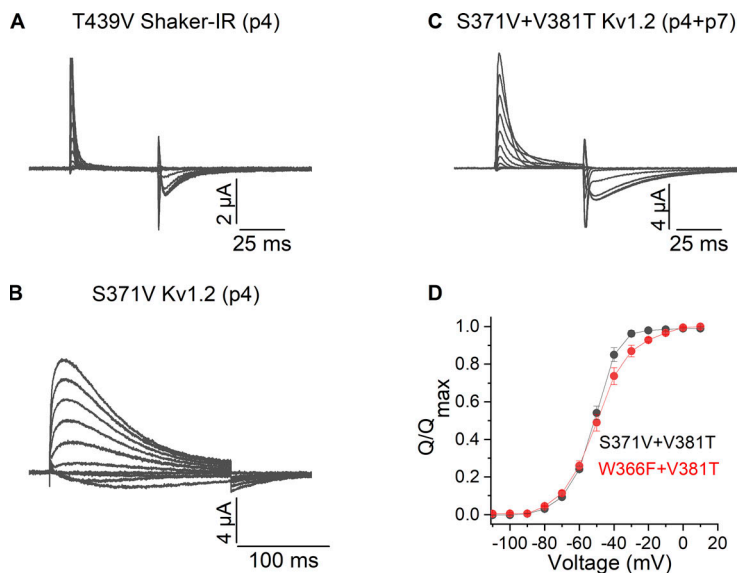
A T439V Shaker-IR (p4)

C S371V+V381T Kv1.2 (p4+p7)

B S371V Kv1.2 (p4)

D

Figure 3. **Ionic and gating currents recordings for mutants at p4 and p7 in the Shaker and Kv1.2 channels. (A)** Family of gating currents for Shaker-IR T439V (p4). **(B)** Family of ionic currents for Kv1.2 S371V (p4). **(C)** Family of gating currents for Kv1.2 S371V/V381T (p4/p7). **(D)** Normalized Q–V relations for Kv1.2 W366F/V381T (p2/p7) and Kv1.2 S371V/V381T (p4/p7). Q was obtained by integrating the ON components of the gating current; all data are mean ± SEM; n = 3 for Kv1.2 W366F/V381T (p2/p7) and n = 5 for Kv1.2 S371V/V381T (p4/p7).

another and their interactions are lost (Fig. 1 F; Tan et al., 2022). These stabilizing interactions seen in the structure of Shaker are also seen in the structure of a conducting state of the Kv1.2/2.1 paddle chimera (Fig. 1 G; Long et al., 2007) and are similarly lost in the structure of a triple mutant (W362F/S367T/V377T; p2/p4/p7) of the Kv1.2/2.1 paddle chimera (Fig. 1 H; Reddi et al., 2022).

Confirming mutant phenotypes at p2 are distinct between Shaker and Kv1.2

For all experiments described here, the Shaker and Kv1.2 channels were expressed without β-subunit in *Xenopus* oocytes and studied using a two-electrode voltage clamp with an external solution containing 50 mM K^+ (see Materials and methods). Previous studies have shown that the W434F (p2) mutant of Shaker is effectively non-conducting because C-type inactivation is very rapid (Yang et al., 1997), and when expressed at sufficiently high levels only gating currents are observed (Perozo et al., 1993), which reflect the movement of the S1–S4 voltage-sensing domains between resting and activated states (Bezanilla, 2018). In Shaker, the T449V (p7) mutant rescues ion conduction in W434F, albeit with faster C-type inactivation compared to Shaker-IR (Yang et al., 2002; Kitaguchi et al., 2004). In contrast to these findings in Shaker, the W366F (p2) mutant in Kv1.2 was reported to be conducting, yet with faster C-type inactivation compared with WT (Suarez-Delgado et al., 2020). Importantly, combining the W366F mutant at p2 in Kv1.2 along with the V381T mutant at p7 to resemble Shaker at that position results in a non-conducting channel (Suarez-Delgado et al., 2020), suggesting that the double mutant has rapid C-type inactivation similar to W434F in Shaker. As a foundation for investigating positions not yet studied in Kv1.2, we repeated these key findings with mutations at p2 and p7, and our results fully confirmed the published findings (Fig. 2). We see that T449V (p7) rescues ion conduction when combined with Shaker W434F (p2; Fig. 2, A, C, and E), and W366F in Kv1.2 is conducting

with more rapid C-type inactivation (Fig. 2 D) compared with WT Kv1.2 (Fig. 2 B), and combining V381T along with W366F in Kv1.2 results in a non-conducting channel where only gating currents are observed (Fig. 2 F). We also attempted to investigate a mutation at the critical Asp at p6 in Kv1.2 (D379N), which in Shaker results in non-conducting channels (Hurst et al., 1996; Pless et al., 2013), but were unable to detect either ion currents or gating currents for this mutant in Kv1.2.

Mutant phenotypes at p4 are distinct between Shaker and Kv1.2

We next investigated mutations at p4, a position where Shaker contains a Thr and Kv1.2 a Ser, each of which forms hydrogen bonds with the Tyr at p5 in structures of Shaker and Kv1.2 in conducting conformations (Fig. 1, E and G). The T439V (p4) mutant in Shaker results in a non-conducting channel, suggesting that it rapidly C-type inactivates (Pless et al., 2013), which we also observed when we expressed the mutant at high levels and observe only gating currents (Fig. 3 A). In contrast, we see that the S371V (p4) mutant in Kv1.2 can conduct, albeit with more rapid C-type inactivation (Fig. 3 B), compared with WT (Fig. 2 B). Similar to phenotypes observed for mutations at p2, when the V381T (p7) mutant is combined with S371V (p4) in Kv1.2, we only observed gating currents when the channel is expressed at high levels (Fig. 3 C), suggesting that the double mutant is non-conducting because it rapidly C-type inactivates. Integration of the gating currents for the double mutant of Kv1.2 yields charge (Q) vs. voltage (V) relations that are similar to those of the W366F/V381T double mutant (Fig. 3 D), which are also not substantially altered compared with gating currents recorded for Shaker or Kv1.2 under other conditions (Bezanilla, 2018). That the residue at p7 determines the phenotypes observed for mutations at both p2 and p4 suggests that p7 is a particularly critical residue capable of influencing how mutations in two distinct hydrogen bond networks influence C-type inactivation.
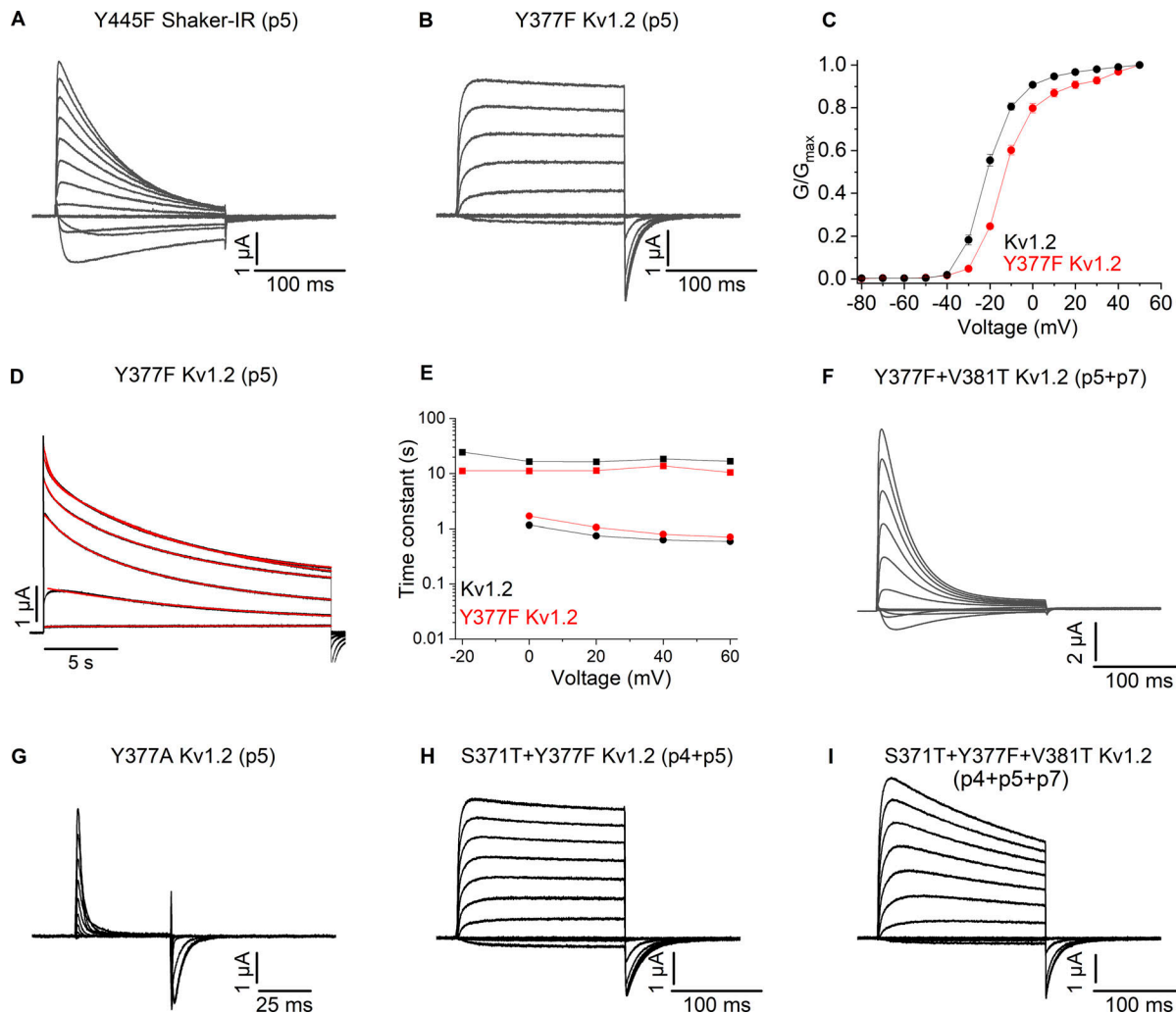
Figure 4. **Ionic and gating currents recordings for mutations at p4, p5, and p7 in the Shaker and Kv1.2 channels. (A)** Family of ionic currents for Shaker-IR Y445F (p5). **(B)** Family of ionic currents for Kv1.2 Y377F (p5). **(C)** G–V relations for Kv1.2 and Kv1.2 Y377F (p5). Normalized G–V relations were obtained by measuring the amplitude of the tail current and normalizing to the maximum elicited following depolarization to +50 mV. n = 6 for Kv1.2 Y377F (p5) and n = 7 for Kv1.2. **(D)** Currents in response to long (20 s) pulses from −20 to +60 mV in 20-mV steps for Kv1.2 Y377F (p5). The current slowly decays in amplitude as a result of a slow inactivation process. The red curves are the fits of a double-exponential function to the current traces. **(E)** Inactivation time constants are plotted as a function of voltage for Kv1.2 and Kv1.2 Y377F (p5). The filled square symbols are slow time constants, and the filled circle are fast time constants. n = 7 for Kv1.2, n = 6 for Kv1.2 Y377F (p5), and n = 5 for Kv1.2 Y377F+V381T (p5/p7). **(F)** Family of ionic currents for Kv1.2 Y377F/V381T (p5/p7). **(G)** Family of gating currents for Kv1.2 Y377A (p5). **(H)** Family of ionic currents for Kv1.2 S371T/Y377F (p4/p5). **(I)** Family of ionic currents for Kv1.2 S371T/Y377F/V381T Kv1.2 (p4/p5/P7). All data are mean ± SEM.

Mutant phenotypes at p5 are distinct between Shaker and Kv1.2

In structures of Shaker and the Kv1.2/2.1 paddle chimera, the Tyr at p5 (Y445 and Y377, respectively) undergoes substantial movement from a position where it interacts with the neighboring subunit in conducting states to rotating behind the SF in the structures of mutants that promote C-type inactivation (Fig. 1; Reddi et al., 2022; Tan et al., 2022). In the conducting states of both channels, the Tyr at p5 hydrogen bonds with the Trp (p3) and Thr/Ser (p4) and contacts Trp (p2) and Thr/Val (p7; Fig. 1, E and G). In previous studies with the Shaker Kv channel, Y445F (p5) is conducting, but displays more rapid C-type inactivation compared with WT (Pless et al., 2013). To confirm earlier findings, we first studied the Y445F (p5) mutant in

Shaker and observed a conducting channel with more rapid C-type inactivation (Fig. 4 A) compared to Shaker-IR (Fig. 2 A), similar to previous results (Pless et al., 2013). In sharp contrast, Y377F (p5) in Kv1.2 exhibits unaltered slow C-type inactivation compared with WT Kv1.2 (Fig. 4, B, D and E). Compared with WT Kv1.2, the conductance (G)–V relation for Y377F (p5) in Kv1.2 is only modestly shifted to more positive voltages (Fig. 4 C), suggesting that the impact of the mutant on voltage-dependent activation cannot explain its low impact on slow inactivation. When activating Y377F with a long (20 s) step to +60 mV, the decay of the ionic current follows a double-exponential time course with time constants of ∼0.8 and 14 s, with the amplitude of the slow component predominating, similar to WT Kv1.2 where time constants of ∼0.6 and 18 s were obtained (Fig. 4, D
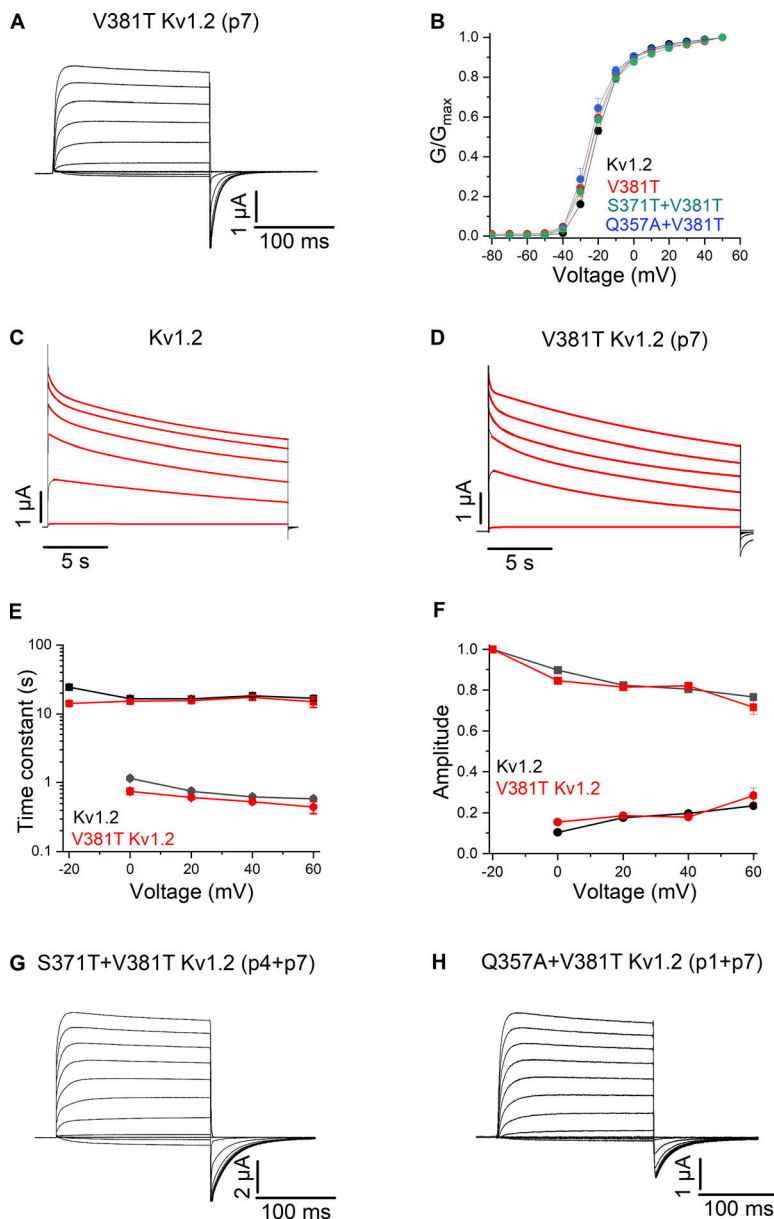
Figure 5. **Ionic currents recordings for mutations at p1, p4, and p7 in the Kv1.2 channel. (A)** Family of ionic currents for Kv1.2 V381T (p7). **(B)** G–V relations for Kv1.2, Kv1.2 V381T (p7), Kv1.2 S371T/V381T (p4/p7), and Kv1.2 Q357A/V381T (p1/p7). Normalized G–V relations were obtained by measuring the amplitude of the tail current and normalizing to the maximum elicited following depolarization to +50 mV. $n = 5$ for Kv1.2 V381T (p7), $n = 5$ for Kv1.2 S371T/V381T (p4/p7), $n = 5$ for Kv1.2 Q357A/V381T (p1/p7), and $n = 7$ for Kv1.2. **(C)** Currents in response to long (20 s) pulses from −20 to +60 mV in 20-mV steps for Kv1.2. The red curve is the fit of a double-exponential function to the current traces. **(D)** Currents in response to long (20 s) pulses from −20 to +60 mV in 20-mV steps for Kv1.2 V381T (p7). **(E)** Inactivation time constants plotted as a function of voltage for Kv1.2 and Kv1.2 V381T (p7). Filled square symbols are slow time constants, and filled circles are fast time constants. $n = 7$ for Kv1.2 and $n = 5$ for Kv1.2 V381T (p7). **(F)** Amplitudes for fast and slow components for Kv1.2 and Kv1.2 V381T (p7). $A_{fast}/(A_{fast} + A_{slow})$ are shown as circles, and the $A_{slow}/(A_{fast} + A_{slow})$ as squares. $n = 7$ for Kv1.2 and $n = 5$ for Kv1.2 V381T (p7). **(G)** Family of ionic currents for Kv1.2 S371T/V381T (p4/p7). **(H)** Family of ionic currents for Kv1.2 Q357A/V381T (p1/p7). All data are mean ± SEM.

and E). In agreement with what was observed for mutations at p2 and p4 in Kv1.2, combining V381T (p7) along with Y377F (p5) resulted in a conducting channel that displayed more rapid C-type inactivation (Fig. 4 F) compared with Y377F alone (Fig. 4 B) or WT Kv1.2 (Fig. 2 B). These findings demonstrate that there are clear quantitative differences between Shaker and Kv1.2 for mutations at p5, and as we found for mutations at p2 and p4, differences between the two channels at p7 seem to account for the different behaviors observed in the two channels.

To explore whether residue differences at p4 (Ser/Thr) might also help to understand the unique phenotypes we observed for mutations at p5, we studied the S371T/Y377F (p4/p5) double mutant and observed a conducting channel with inactivation properties similar to Y377F alone (Fig. 4, B and H) or to the WT Kv1.2 channel (Fig. 2 B). We also studied a triple mutant of Kv1.2 containing mutations at p5, p7, and p4 (Y377F, V381T, and S371T) and observed a conducting channel with slightly faster

inactivation compared to WT, Y377F (p5), or S371T/Y377F (p4/p5; Fig. 4 I), suggesting that differences between Shaker and Kv1.2 at p4 do not play an important role in the phenotypic differences observed between the two channels.

In previous studies on Shaker, the aromatic ring of the Tyr (p5) is essential for maintaining the open state as its mutation to Ala results in non-conducting channels where gating currents can be readily measured even though there is no evidence of ion conduction (Pless et al., 2013). To explore whether an aromatic ring is also essential for Kv1.2, we studied the Y377A (p5) mutant and observed that the channel is non-conducting and only gating currents can be recorded (Fig. 4 G), indicating that the aromatic ring of the Tyr (p5) is a key factor in maintaining the open state of both Shaker and the Kv1.2 channel.

The final position structurally implicated in hydrogen bonding with p5 in both Shaker and Kv1.2 is p3. Although the W435F p3 mutant in Shaker does not dramatically alter C-type
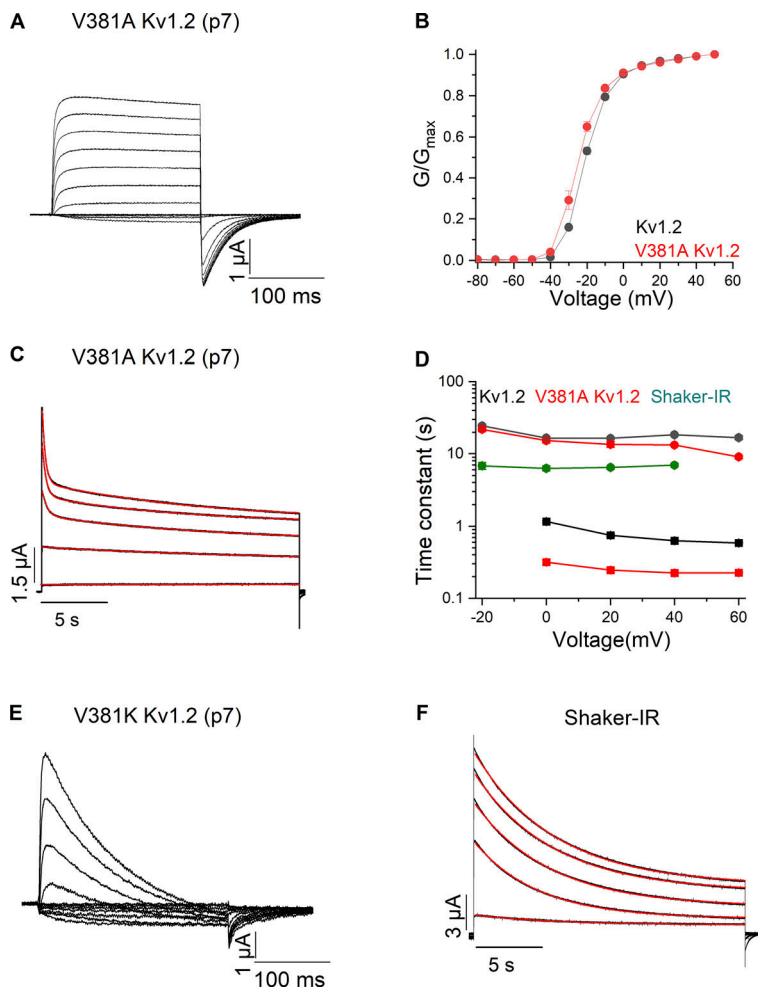
Wu et al.
Comparing slow inactivation in Kv1 channels

A V381A Kv1.2 (p7)

B

C V381A Kv1.2 (p7)

D

E V381K Kv1.2 (p7)

F Shaker-IR

Figure 6. **Ionic currents recordings for mutations at p7 in the Kv1.2 channel. (A)** Family of ionic currents for Kv1.2 V381A (p7). **(B)** G–V relations for Kv1.2 and Kv1.2 V381A (p7). Normalized G–V relations were obtained by measuring the amplitude of the tail current and normalizing to the maximum elicited following depolarization to +50 mV. n = 5 for Kv1.2 V381A (p7) and n = 7 for Kv1.2. **(C)** Currents in response to long (20 s) pulses from −20 to +60 mV in 20-mV steps for Kv1.2 V381A (p7). The red curve is the fit of a double-exponential function to the current traces. **(D)** Inactivation time constants plotted as a function of voltage for Kv1.2, Kv1.2 V381A (p7), and Shaker-IR. The filled square symbols are slow time constants, and the filled circles are fast time constants. n = 7 for Kv1.2, n = 5 for Kv1.2 V381A (p7) and n = 5 for Shaker-IR. **(E)** Family of ionic currents for Kv1.2 V381K (p7). **(F)** Currents in response to long (20 s) pulses from −20 to +40 mV in 20 mV steps for Shaker-IR. The red curve is the fit of a single-exponential function to the current traces.

inactivation (Pless et al., 2013), to exclude the possibility that some mutations are more impactful in Kv1.2, we mutated the corresponding p3 residue in Kv1.2 (W367F). As in Shaker, the p3 mutant in Kv1.2 remains conducting and slow inactivates with similar properties compared with the WT channel (Fig. 7, A and B).

Mutant phenotypes at p7 are distinct between Shaker and Kv1.2

One of the general themes emerging from the results thus far is that p7 plays a critical role in determining the impact of mutations at the most conserved positions studied. Mutation of p7 from Val to Thr renders the impact of p2, p4, and p5 mutations similar for Kv1.2 channels when compared to Shaker. One explanation that would be consistent with all our results would be to posit that Kv1.2 is more resistant to inactivation when compared with Shaker, with Val at p7 being one determinant responsible for Kv1.2 resisting inactivation. Recalling that substitutions at T449 (p7) in Shaker with more hydrophobic residues like Val dramatically slow C-type inactivation (Lopez-Barneo et al., 1993), we next assessed the individual impact of mutations at p7 (V381) in Kv1.2 by initially mutating that position to Thr, expecting, based on studies in Shaker (Lopez-Barneo et al., 1993), to observe faster slow inactivation. Surprisingly,

however, we found that ionic currents recorded for V381T exhibited slow C-type inactivation and a G–V relation that were both quite similar to WT Kv1.2 channel (Fig. 5, A–F). We also combined the V381T (p7) mutation along with the S371T (p4) mutation and observed similar results (Fig. 5, B and G). These findings demonstrate that when studied in isolation, the p7 position has a much greater impact on slow inactivation in Shaker (Lopez-Barneo et al., 1993) compared with Kv1.2.

From the available structures of Shaker and Kv1.2, we identified an additional residue difference at p1 that is positioned near p7 and could conceivably have a local influence on mutations at p7. At p1, Shaker contains a Phe (F425) known to influence the binding of pore-blocking scorpion toxins (Goldstein and Miller, 1992; Goldstein et al., 1994), and Kv1.2 contains a polar Gln. Although the Q357F (p1) mutant in Kv1.2 failed to give rise to functional channels (no ionic or gating currents could be observed), combining the Q357A mutant at p1 along with V381T (p7) did not dramatically speed C-type inactivation in Kv1.2 (Fig. 5, B and H). As the more drastic T449A and T449K mutations at p7 in Shaker accelerate C-type inactivation by about eightfold and 32-fold (Lopez-Barneo et al., 1993), respectively, we tested whether the corresponding mutations in Kv1.2 might have more readily detectable effects on C-type inactivation. Although relatively short ionic current traces for the V381A (p7)
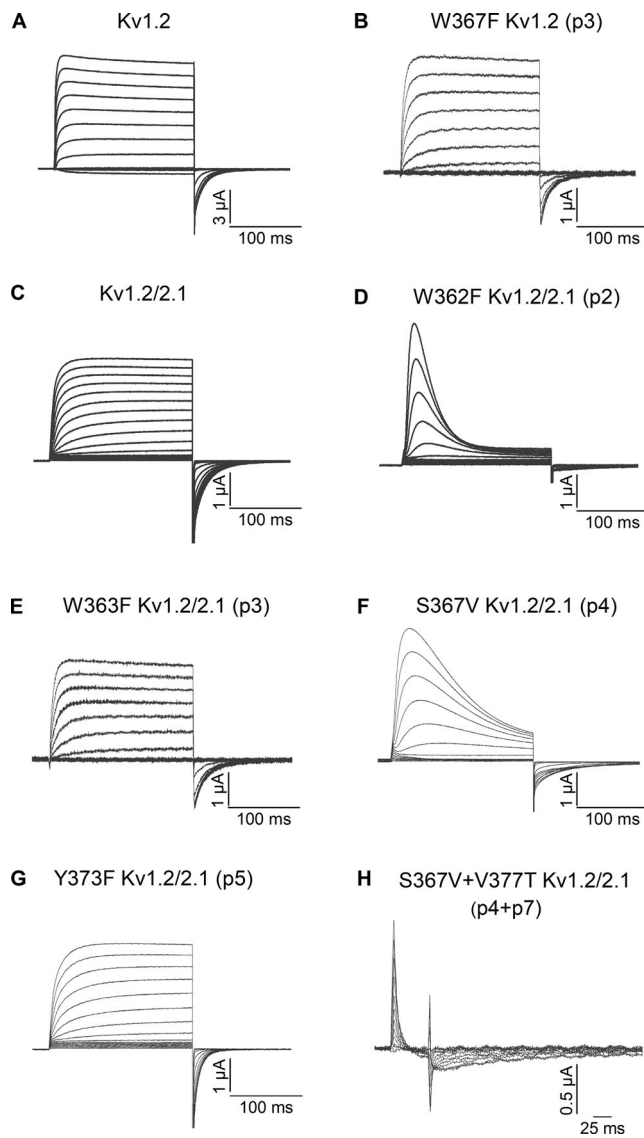
Figure 7. **Ionic and gating currents recordings for Kv1.2 and the Kv1.2/2.1 paddle chimera as well as their mutants at p2, p3, p4, p6, and p7.** **(A)** Family of ionic currents for Kv1.2. **(B)** Family of ionic currents for Kv1.2 W367F (p3). **(C)** Family of ionic currents for the Kv1.2/2.1 paddle chimera. **(D)** Family of ionic currents for Kv1.2/2.1 W362F (p2). **(E)** Family of ionic currents for Kv1.2/2.1 W363F (p3). **(F)** Family of ionic currents for Kv1.2/2.1 S367V (p4). **(G)** Family of ionic currents for Kv1.2/2.1 Y373F (p5). **(H)** Family of gating currents for Kv1.2/2.1 S367V/V381T (p4/p7).

mutant in Kv1.2 are similar to the WT Kv1.2 on first inspection (Fig. 6 A), with a relatively unperturbed G–V relation (Fig. 6 B), longer pulses reveal that the mutant accelerates the fast component of inactivation by about threefold (Fig. 6, C and D) compared with the WT Kv1.2 channel. In contrast, the V381K (p7) mutant clearly exhibited accelerated C-type inactivation (Fig. 6 E), albeit to a lesser extent, than that observed in Shaker. We also compared slow C-type inactivation in Shaker and Kv1.2 channels under our recording conditions. Although slow inactivation in Shaker can be reasonably well described with a single exponential function (Fig. 6 F), whereas Kv1.2 requires a double exponential function (Fig. 5 C), the time constants for

inactivation in Shaker are around threefold faster than the most prominent slow component of inactivation in Kv1.2 (Fig. 6 D). Taken together, our results reveal that mutations near the SF expected to disrupt side-chain interactions that stabilize the conducting states of both channels (Fig. 1, E and G) consistently have a more substantial energetic impact on Shaker when compared with Kv1.2. Either the conducting state in Kv1.2 is intrinsically more stable compared with Shaker or the energy barrier for entry into the inactivated state is higher.

Mutant phenotypes in Kv1.2 and the Kv1.2/2.1 paddle chimera are similar

As the x-ray structure of the Kv1.2/2.1 paddle chimera has been an important foundation for exploring Kv channel mechanisms (Long et al., 2007), and the recent structure of the Kv1.2/2.1 paddle chimera with three additional mutations (at p2, p4, and p7) supports a mechanism for slow inactivation involving dilation at the external end of the SF (Reddi et al., 2022), we tested whether our findings with Kv1.2 are also applicable for the chimera. The W362F mutation at p2 in the chimera resulted in a conducting channel with rapid C-type inactivation (Fig. 7, C and D), similar to what has been observed in Kv1.2 (Suarez-Delgado et al., 2020; Fig. 2 D). As found in Shaker and Kv1.2, the W363F mutation at p3 did not substantially alter slow inactivation (Fig. 7 E). The S367V mutation at p4 produced a conducting channel with relatively rapid C-type inactivation (Fig. 7 F), not unlike what we observed in Kv1.2 (Fig. 4 B). Moreover, the Y373F mutation at p5 did not appreciably alter C-type inactivation (Fig. 7 G), similar to what we observed in Kv1.2 but very different from what is seen in Shaker (Pless et al., 2013; Fig. 4, A and B). Finally, we tested the additional mutation at p7 (V377T) together with that at p4 (S367V) in the chimera, and although this construct expressed very poorly, when currents could be recorded, we observed a non-conducting phenotype where only gating currents could be observed (Fig. 7 H), again reminiscent of what we observed in Kv1.2 (Fig. 3 C). This comparison suggests that the Kv1.2/2.1 paddle chimera behaves similar to Kv1.2 and therefore is a valid structural target for interrogating mechanisms of slow inactivation in Kv1.2.

Discussion

The objective of the present study was to systematically compare the impact of mutations at key positions near the SF of Shaker and Kv1.2 channels to understand how their mechanisms of slow inactivation are related. Each of the positions studied is involved in a hydrogen bond network that stabilizes the conducting state of both channels. For p2, p4, and p5, mutations that dramatically speed inactivation in Shaker have consistently less robust influence on slow inactivation in Kv1.2 (Table 2). In each of these cases, however, the severity of the impact of mutations at p2, p4, and p5 in Kv1.2 resembles that observed in Shaker when combined with a mutation at p7 from Val to Thr (Table 2). In structures thought to represent conducting states of both Shaker and Kv1.2, the Trp at p2 hydrogen bonds with the Asp at p6, the Tyr at p5 hydrogen bonds with the Trp at p3 and the Ser/Thr at p4, and the Thr/Val at p7 is close enough to the Tyr at p5 to have

Table 2. The functional effects of Shaker and Kv1.2 mutations

	Shaker	Functional effect	Kv1.2	Functional effect
WT	W434	Conducting	W366	Conducting
p2	W434F	Non-conducting	W366F	Faster inactivation
p3	W435F	Conducting	W367F	Conducting
p4	T439V	Non-conducting	S371V	Faster inactivation
p5	Y445F	Faster inactivation	Y377F	Conducting
	Y445A	Non-conducting	Y377A	Non-conducting
p6	D447N	Non-conducting	D379N	Non-functional channel
p7	T449V	Slower inactivation	V381T	Conducting
	T449A	Faster inactivation	V381A	Faster inactivation
	T449K	Faster inactivation	V381K	Faster inactivation
p1/p7			Q357A/V381T	Conducting
p2/p7	W434F/T449	Faster inactivation	W366F/V381T	Non-conducting
p4/p5			S371T/Y377F	Conducting
p4/p5/p7			S371T/Y377F/V381T	Faster inactivation
p4/p7			S371V/V381T	Non-conducting
			S371T/V381T	Conducting
p5/p7			Y377F/V381T	Faster inactivation

a hydrophobic interaction (Fig. 1, E and G). In mutant structures of both channels proposed to represent a slow C-type inactivated state (Fig. 1, F and H), the Tyr at p5 undergoes a large displacement to rotate outward behind the SF, leading to its dilation and breaking off its hydrogen bonds with the Trp at p3 and the Ser/Thr at p4 and its hydrophobic interaction with the Thr/Val at p7, residing between the Trp at p2 and the Asp at p6. Thus, the Tyr at p5 is central to the reorganization behind the SF accompanying dilation of the SF that occurs during inactivation in both Shaker and Kv1.2 channels. If the structures of Shaker and Kv1.2 faithfully capture the conformational change that occurs with C-type inactivation, we would anticipate observing similar structural changes in the T439V (p4) and Y445A (p5) mutants of Shaker, as both are effectively non-conducting (Figs. 3 and 4; Table 2). As the available structure of WT Shaker was obtained in the presence of high K+ concentrations (Tan et al., 2022), and high K+ slows inactivation (Lopez-Barneo et al., 1993), it might also be possible to capture a dilated SF for the WT Shaker Kv channel in the presence of low K+ concentration.

That the Thr/Val differences at p7 between Shaker and Kv1.2 critically determine the phenotypes observed for mutations at p2, p4, and p5 suggest that the hydrophobic interactions between the Thr/Val at p7 and the Tyr p5 are a critical determinant of how mutations influence slow inactivation in the two channels. However, it is also interesting that individual mutations at p7 have a much stronger influence on slow inactivation in Shaker compared with Kv1.2, suggesting that either the conducting state of Kv1.2 is intrinsically more stable than Shaker when compared with the inactivated state or the energy barrier between conducting and inactivated states is considerably higher in Kv1.2, irrespective of the residue present at the p7 position. The resistance of Kv1.2 to inactivate can explain why it has been challenging to solve structures of this channel in an

inactivated state (Pau et al., 2017; Matthies et al., 2018). Although the sequence identity between Shaker and Kv1.2 is high around the SF, there are many positions that vary between the two channels in the sequence between S5 and S6 that forms the SF (Fig. 1 A) and in the outer end of the S6 helix that cradles the SF in the outer pore of the channel.

The mechanism of slow inactivation in Kv1.3 is also germane to the present comparison of slow inactivation in Shaker and Kv1.2 channels. The W436F mutation at p2 in hKv1.3 renders the channel non-conducting (Kubota et al., 2017) much like the corresponding W434F mutation in Shaker. In addition, although the D402N mutation at p6 was reported to not form functional channels, concatenated dimers with WT and the D402N mutation are conducting with faster inactivation (Aiyar et al., 1996), a result that is similar to what is observed for D447N mutations in the Shaker Kv channel (Pless et al., 2013). Mutations at p7, which in Kv1.3 is a His, influence inactivation similarly to what is observed in Shaker (Busch et al., 1991; Nguyen et al., 1996; Jager et al., 1998; Somodi et al., 2004). Recent structures of Kv1.3 channels captured in inactivated states also display a dilated SF, similar to what is seen in the Shaker and Kv1.2 channels, but where distinct conformations are observed that may reflect intermediates between conducting and inactivated states (Selvakumar et al., 2022; Tyagi et al., 2022). All of the structural studies in Shaker, Kv1.2, and Kv1.3 used high K+ concentrations (Reddi et al., 2022; Selvakumar et al., 2022; Tan et al., 2022; Tyagi et al., 2022), which interferes with inactivation (Lopez-Barneo et al., 1993), explaining why both Shaker and Kv1.2 were captured with the SF in a conducting state in the absence of inactivation-promoting mutations (Reddi et al., 2022; Tan et al., 2022). Importantly, inactivated conformations of the SF in Kv1.3 were observed in elevated K+ solutions, and conducting conformations were only observed with inhibitors bound to

stabilize that conformation (Selvakumar et al., 2022; Tyagi et al., 2022). This comparison would suggest that Shaker, Kv1.2, and Kv1.3 have similar mechanisms of inactivation, yet with important energic differences that make Kv1.3 the most prone to inactivate, followed by Shaker, and then Kv1.2 being the most resistant. It will be interesting to study other Kv1 channels to see whether their slow inactivation mechanisms fit with what we have learned thus far from studies on Shaker, Kv1.2, and Kv1.3. The Kv1.5 channel is rendered non-conducting by the W472F mutation at p2 (Chen et al., 1997), for example, yet contains an Arg (R487) at p7 and retains slow inactivation even when this position is mutated to Val or Tyr (Fedida et al., 1999).

The family of Kv channels is large and diverse and the mechanisms of inactivation are only coming into focus for a few Kv1 channels. It will be interesting to understand whether dilation of the SF is a mechanism common to other Kv channels or to other types of K+ channels where a dynamic SF plays an important role in channel gating (Zilberberg et al., 2001; Bagriantsev et al., 2011; Yan et al., 2016; Lolicato et al., 2020). One might speculate that other mechanisms of inactivation are important, for example, like that described in the KcsA K+ channel where the SF appears to collapse during inactivation (Cuello et al., 2017). One notable example might be the Kv2.1 channel, where slow inactivation is not very sensitive to external K+, blockers such as tetraethylammonium, or mutations near the SF (Klemic et al., 1998; Carrillo et al., 2013; Jamieson and Jones, 2013). However, the different mutant phenotypes observed here when comparing the closely related Shaker and Kv1.2 channels would suggest that distinct mutant phenotypes are not necessarily an indication of different mechanisms of slow inactivation. It will be exciting to solve structures of other K+ channels under conditions favoring inactivated conformations of the SF to further explore mechanisms of inactivation.

Acknowledgments

References

Adelman, J.P., C.T. Bond, M. Pessia, and J. Maylie. 1995. Episodic ataxia results from voltage-dependent potassium channels with altered functions. *Neuron*. 15:1449–1454. https://doi.org/10.1016/0896-6273(95)90022-5

Aiyar, J., J.P. Rizzi, G.A. Gutman, and K.G. Chandy. 1996. The signature sequence of voltage-gated potassium channels projects into the external vestibule. *J. Biol. Chem.* 271:31013–31016. https://doi.org/10.1074/jbc.271.49.31013

Alabi, A.A., M.I. Bahamonde, H.J. Jung, J.I. Kim, and K.J. Swartz. 2007. Portability of paddle motif function and pharmacology in voltage sensors. *Nature*. 450:370–375. https://doi.org/10.1038/nature06266

Bagriantsev, S.N., R. Peyronnet, K.A. Clark, E. Honore, and D.L. Minor Jr. 2011. Multiple modalities converge on a common gate to control K2P channel function. *EMBO J.* 30:3594–3606. https://doi.org/10.1038/emboj.2011.230

Baukrowitz, T., and G. Yellen. 1995. Modulation of K+ current by frequency and external [K+]: A tale of two inactivation mechanisms. *Neuron*. 15:951–960. https://doi.org/10.1016/0896-6273(95)90185-x

Bezanilla, F. 2008. How membrane proteins sense voltage. *Nat. Rev. Mol. Cell Biol.* 9:323–332. https://doi.org/10.1038/nrm2376

Bezanilla, F. 2018. Gating currents. *J. Gen. Physiol.* 150:911–932. https://doi.org/10.1085/jgp.201812090

Busch, A.E., R.S. Hurst, R.A. North, J.P. Adelman, and M.P. Kavanaugh. 1991. Current inactivation involves a histidine residue in the pore of the rat lymphocyte potassium channel RGK5. *Biochem. Biophys. Res. Commun.* 179:1384–1390. https://doi.org/10.1016/0006-291x(91)91726-s

Carrillo, E., I.I.Arias-Olguín, L.D. Islas, F. Gómez-Lagunas, and F. Gomez-Lagunas. 2013. Shab K (+) channel slow inactivation: A test for U-type inactivation and a hypothesis regarding K (+) -facilitated inactivation mechanisms. *Channels*. 7:97–108. https://doi.org/10.4161/chan.23569

Chen, F.S., D. Steele, and D. Fedida. 1997. Allosteric effects of permeating cations on gating currents during K+ channel deactivation. *J. Gen. Physiol.* 110:87–100. https://doi.org/10.1085/jgp.110.2.87

Choi, K.L., R.W. Aldrich, and G. Yellen. 1991. Tetraethylammonium blockade distinguishes two inactivation mechanisms in voltage-activated K+ channels. *Proc. Natl. Acad. Sci. USA.* 88:5092–5095. https://doi.org/10.1073/pnas.88.12.5092

Cuello, L.G., D.M. Cortes, and E. Perozo. 2017. The gating cycle of a K(+) channel at atomic resolution. *Elife*. 6:e28032. https://doi.org/10.7554/eLife.28032

del Camino, D., M. Holmgren, Y. Liu, and G. Yellen. 2000. Blocker protection in the pore of a voltage-gated K+ channel and its structural implications. *Nature*. 403:321–325. https://doi.org/10.1038/35002099

del Camino, D., and G. Yellen. 2001. Tight steric closure at the intracellular activation gate of a voltage- gated k(+) channel. *Neuron*. 32:649–656. https://doi.org/10.1016/s0896-6273(01)00487-1

Doyle, D.A., J. Morais Cabral, R.A. Pfuetzner, A. Kuo, J.M. Gulbis, S.L. Cohen, B.T. Chait, and R. MacKinnon. 1998. The structure of the potassium channel: Molecular basis of K+ conduction and selectivity. *Science*. 280:69–77. https://doi.org/10.1126/science.280.5360.69

Fedida, D., N.D. Maruoka, and S. Lin. 1999. Modulation of slow inactivation in human cardiac Kv1.5 channels by extra- and intracellular permeant cations. *J. Physiol.* 515 (Pt 2):315–329. https://doi.org/10.1111/j.1469-7793.1999.315ac.x

Goldstein, S.A., and C. Miller. 1992. A point mutation in a Shaker K+ channel changes its charybdotoxin binding site from low to high affinity. *Biophys. J.* 62:5–7. https://doi.org/10.1016/S0006-3495(92)81760-5

Goldstein, S.A., D.J. Pheasant, and C. Miller. 1994. The charybdotoxin receptor of a shaker K+ channel: Peptide and channel residues mediating molecular recognition. *Neuron*. 12:1377–1388. https://doi.org/10.1016/0896-6273(94)90452-9

Heginbotham, L., Z. Lu, T. Abramson, and R. MacKinnon. 1994. Mutations in the K+ channel signature sequence. *Biophys. J.* 66:1061–1067. https://doi.org/10.1016/S0006-3495(94)80887-2

Holmgren, M., K.S. Shin, and G. Yellen. 1998. The activation gate of a voltage-gated K+ channel can be trapped in the open state by an intersubunit metal bridge. *Neuron*. 21:617–621. https://doi.org/10.1016/s0896-6273(00)80571-1

Holmgren, M., P.L. Smith, and G. Yellen. 1997. Trapping of organic blockers by closing of voltage-dependent K+ channels: Evidence for a trap door mechanism of activation gating. *J. Gen. Physiol.* 109:527–535. https://doi.org/10.1085/jgp.109.5.527

Hoshi, T., and C.M. Armstrong. 2013. C-Type inactivation of voltage-gated K+ channels: Pore constriction or dilation? *J. Gen. Physiol.* 141:151–160. https://doi.org/10.1085/jgp.201210888

Hoshi, T., W.N. Zagotta, and R.W. Aldrich. 1990. Biophysical and molecular mechanisms of Shaker potassium channel inactivation. *Science*. 250:533–538. https://doi.org/10.1126/science.2122519

Hoshi, T., W.N. Zagotta, and R.W. Aldrich. 1991. Two types of inactivation in shaker K+ channels: Effects of alterations in the carboxy-terminal region. *Neuron*. 7:547–556. https://doi.org/10.1016/0896-6273(91)90367-9

Hubner, C.A., and T.J. Jentsch. 2002. Ion channel diseases. *Hum. Mol. Genet.* 11:2435–2445. https://doi.org/10.1093/hmg/11.20.2435

Hurst, R.S., L. Toro, and E. Stefani. 1996. Molecular determinants of external barium block in Shaker potassium channels. *FEBS Lett.* 388:59–65. https://doi.org/10.1016/0014-5793(96)00516-9

Jager, H., H. Rauer, A.N. Nguyen, J. Aiyar, K.G. Chandy, and S. Grissmer. 1998. Regulation of mammalian shaker-related K+ channels: Evidence for non-conducting closed and non-conducting inactivated states. *J. Physiol.* 506 (Pt 2):291–301. https://doi.org/10.1111/j.1469-7793.1998.291bw.x

Jamieson, Q., and S.W. Jones. 2013. Role of outer-pore residue Y380 in U-type inactivation of KV2.1 channels. *J. Membr. Biol.* 246:633–645. https://doi.org/10.1007/s00232-013-9577-0

Jan, L.Y., and Y.N. Jan. 2012. Voltage-gated potassium channels and the diversity of electrical signalling. *J. Physiol.* 590:2591–2599. https://doi.org/10.1113/jphysiol.2011.224212

Kitaguchi, T., M. Sukhareva, and K.J. Swartz. 2004. Stabilizing the closed S6 gate in the Shaker Kv channel through modification of a hydrophobic seal. *J. Gen. Physiol.* 124:319–332. https://doi.org/10.1085/jgp.200409098

Klemic, K.G., C.C. Shieh, G.E. Kirsch, and S.W. Jones. 1998. Inactivation of Kv2.1 potassium channels. *Biophys. J.* 74:1779–1789. https://doi.org/10.1016/S0006-3495(98)77888-9

Kubota, T., A.M. Correa, and F. Bezanilla. 2017. Mechanism of functional interaction between potassium channel Kv1.3 and sodium channel NavBeta1 subunit. *Sci. Rep.* 7:45310. https://doi.org/10.1038/srep45310

Kurata, H.T., and D. Fedida. 2006. A structural interpretation of voltage-gated potassium channel inactivation. *Prog. Biophys. Mol. Biol.* 92:185–208. https://doi.org/10.1016/j.pbiomolbio.2005.10.001

Liman, E.R., J. Tytgat, and P. Hess. 1992. Subunit stoichiometry of a mammalian K+ channel determined by construction of multimeric cDNAs. *Neuron.* 9:861–871. https://doi.org/10.1016/0896-6273(92)90239-a

Liu, Y., M. Holmgren, M.E. Jurman, and G. Yellen. 1997. Gated access to the pore of a voltage-dependent K+ channel. *Neuron.* 19:175–184. https://doi.org/10.1016/s0896-6273(00)80357-8

Liu, Y., M.E. Jurman, and G. Yellen. 1996. Dynamic rearrangement of the outer mouth of a K+ channel during gating. *Neuron.* 16:859–867. https://doi.org/10.1016/s0896-6273(00)80106-3

Lolicato, M., A.M. Natale, F. Abderemane-Ali, D. Crottes, S. Capponi, R. Duman, A. Wagner, J.M. Rosenberg, M. Grabe, and D.L. Minor Jr. 2020. K2P channel C-type gating involves asymmetric selectivity filter order-disorder transitions. *Sci. Adv.* 6:eabc9174. https://doi.org/10.1126/sciadv.abc9174

Long, S.B., E.B. Campbell, and R. Mackinnon. 2005a. Crystal structure of a mammalian voltage-dependent Shaker family K+ channel. *Science.* 309:897–903. https://doi.org/10.1126/science.1116269

Long, S.B., E.B. Campbell, and R. Mackinnon. 2005b. Voltage sensor of Kv1.2: Structural basis of electromechanical coupling. *Science.* 309:903–908. https://doi.org/10.1126/science.1116270

Long, S.B., X. Tao, E.B. Campbell, and R. MacKinnon. 2007. Atomic structure of a voltage-dependent K+ channel in a lipid membrane-like environment. *Nature.* 450:376–382. https://doi.org/10.1038/nature06265

Lopez-Barneo, J., T. Hoshi, S.H. Heinemann, and R.W. Aldrich. 1993. Effects of external cations and mutations in the pore region on C-type inactivation of Shaker potassium channels. *Recept. Channel.* 1:61–71.

MacKinnon, R. 1991. Determination of the subunit stoichiometry of a voltage-activated potassium channel. *Nature.* 350:232–235. https://doi.org/10.1038/350232a0

MacKinnon, R., and G. Yellen. 1990. Mutations affecting TEA blockade and ion permeation in voltage- activated K+ channels. *Science.* 250:276–279. https://doi.org/10.1126/science.2218530

Matthies, D., C. Bae, G.E. Toombes, T. Fox, A. Bartesaghi, S. Subramaniam, and K.J. Swartz. 2018. Single-particle cryo-EM structure of a voltage-activated potassium channel in lipid nanodiscs. *Elife.* 7:e37558. https://doi.org/10.7554/eLife.37558

Molina, A., A.G. Castellano, and J. Lopez-Barneo. 1997. Pore mutations in Shaker K+ channels distinguish between the sites of tetraethylammonium blockade and C-type inactivation. *J. Physiol.* 499 (Pt 2):361–367. https://doi.org/10.1113/jphysiol.1997.sp021933

Nguyen, A., J.C. Kath, D.C. Hanson, M.S. Biggers, P.C. Canniff, C.B. Donovan, R.J. Mather, M.J. Bruns, H. Rauer, J. Aiyar, et al. 1996. Novel nonpeptide agents potently block the C-type inactivated conformation of Kv1.3 and suppress T cell activation. *Mol. Pharmacol.* 50:1672–1679

Ogielska, E.M., and R.W. Aldrich. 1998. A mutation in S6 of Shaker potassium channels decreases the K+ affinity of an ion binding site revealing ion-ion interactions in the pore. *J. Gen. Physiol.* 112:243–257. https://doi.org/10.1085/jgp.112.2.243

Ogielska, E.M., and R.W. Aldrich. 1999. Functional consequences of a decreased potassium affinity in a potassium channel pore. Ion interactions and c-type inactivation. *J. Gen. Physiol.* 113:347–358. https://doi.org/10.1085/jgp.113.2.347

Papazian, D.M., T.L. Schwarz, B.L. Tempel, L.C. Timpe, and L.Y. Jan. 1988. Ion channels in Drosophila. *Annu. Rev. Physiol.* 50:379–394. https://doi.org/10.1146/annurev.ph.50.030188.002115

Pau, V., Y. Zhou, Y. Ramu, Y. Xu, and Z. Lu. 2017. Crystal structure of an inactivated mutant mammalian voltage-gated K(+) channel. *Nat. Struct. Mol. Biol.* 24:857–865. https://doi.org/10.1038/nsmb.3457

Perozo, E., R. MacKinnon, F. Bezanilla, and E. Stefani. 1993. Gating currents from a nonconducting mutant reveal open-closed conformations in Shaker K+ channels. *Neuron.* 11:353–358. https://doi.org/10.1016/0896-6273(93)90190-3

Pless, S.A., J.D. Galpin, A.P. Niciforovic, H.T. Kurata, and C.A. Ahern. 2013. Hydrogen bonds as molecular timers for slow inactivation in voltage-gated potassium channels. *Elife.* 2:e01289. https://doi.org/10.7554/eLife.01289

Reddi, R., K. Matulef, E.A. Riederer, M.R. Whorton, and F.I. Valiyaveetil. 2022. Structural basis for C-type inactivation in a Shaker family voltage-gated K(+) channel. *Sci. Adv.* 8:eabm8804. https://doi.org/10.1126/sciadv.abm8804

Rettig, J., S.H. Heinemann, F. Wunder, C. Lorra, D.N. Parcej, J.O. Dolly, and O. Pongs. 1994. Inactivation properties of voltage-gated K+ channels altered by presence of beta-subunit. *Nature.* 369:289–294. https://doi.org/10.1038/369289a0

Selvakumar, P., A.I. Fernandez-Marino, N. Khanra, C. He, A.J. Paquette, B. Wang, R. Huang, V.V. Smider, W.J. Rice, K.J. Swartz, and J.R. Meyerson. 2022. Structures of the T cell potassium channel Kv1.3 with immunoglobulin modulators. *Nat. Commun.* 13:3854. https://doi.org/10.1038/s41467-022-31285-5

Somodi, S., Z. Varga, P. Hajdu, J.G. Starkus, D.I. Levy, R. Gaspar, and G. Panyi. 2004. pH-dependent modulation of Kv1.3 inactivation: Role of His399. *Am. J. Physiol. Cell Physiol.* 287:C1067–C1076. https://doi.org/10.1152/ajpcell.00438.2003

Starkus, J.G., L. Kuschel, M.D. Rayner, and S.H. Heinemann. 1997. Ion conduction through C-type inactivated Shaker channels. *J. Gen. Physiol.* 110:539–550. https://doi.org/10.1085/jgp.110.5.539

Suarez-Delgado, E., T.G. Rangel-Sandin, I.G. Ishida, G.E. Rangel-Yescas, T. Rosenbaum, and L.D. Islas. 2020. KV1.2 channels inactivate through a mechanism similar to C-type inactivation. *J. Gen. Physiol.* 152:e201912499. https://doi.org/10.1085/jgp.201912499

Swartz, K.J. 2008. Sensing voltage across lipid membranes. *Nature.* 456:891–897. https://doi.org/10.1038/nature07620

Tan, X.F., C. Bae, R. Stix, A.I. Fernandez-Marino, K. Huffer, T.H. Chang, J. Jiang, J.D. Faraldo-Gomez, and K.J. Swartz. 2022. Structure of the Shaker Kv channel and mechanism of slow C-type inactivation. *Sci. Adv.* 8:eabm7814. https://doi.org/10.1126/sciadv.abm7814

Tyagi, A., T. Ahmed, S. Jian, S. Bajaj, S.T. Ong, S.S.M. Goay, Y. Zhao, I. Vorobyov, C. Tian, K.G. Chandy, and S. Bhushan. 2022. Rearrangement of a unique Kv1.3 selectivity filter conformation upon binding of a drug. *Proc. Natl. Acad. Sci. USA.* 119:e2113536119. https://doi.org/10.1073/pnas.2113536119

Wulff, H., N.A. Castle, and L.A. Pardo. 2009. Voltage-gated potassium channels as therapeutic targets. *Nat. Rev. Drug Discov.* 8:982–1001. https://doi.org/10.1038/nrd2983

Yan, J., Q. Li, and R.W. Aldrich. 2016. Closed state-coupled C-type inactivation in BK channels. *Proc. Natl. Acad. Sci. USA.* 113:6991–6996. https://doi.org/10.1073/pnas.1607584113

Yang, Y., Y. Yan, and F.J. Sigworth. 1997. How does the W434F mutation block current in Shaker potassium channels? *J. Gen. Physiol.* 109:779–789. https://doi.org/10.1085/jgp.109.6.779

Yang, Y., Y. Yan, and F.J. Sigworth. 2002. The Shaker mutation T449V rescues ionic currents of W434F K+ channels. *Biophys. J.* 82:234e

Yellen, G. 2002. The voltage-gated potassium channels and their relatives. *Nature.* 419:35–42. https://doi.org/10.1038/nature00978

Yellen, G., D. Sodickson, T.Y. Chen, and M.E. Jurman. 1994. An engineered cysteine in the external mouth of a K+ channel allows inactivation to be modulated by metal binding. *Biophys. J.* 66:1068–1075. https://doi.org/10.1016/S0006-3495(94)80888-4

Zagotta, W.N., T. Hoshi, and R.W. Aldrich. 1990. Restoration of inactivation in mutants of Shaker potassium channels by a peptide derived from ShB. *Science.* 250:568–571. https://doi.org/10.1126/science.2122520

Zhou, Y., J.H. Morais-Cabral, A. Kaufman, and R. MacKinnon. 2001. Chemistry of ion coordination and hydration revealed by a K+ channel- Fab complex at 2.0 A resolution. *Nature.* 414:43–48. https://doi.org/10.1038/35102009

Zilberberg, N., N. Ilan, and S.A. Goldstein. 2001. KCNKO: Opening and closing the 2-P-domain potassium leak channel entails "C-type" gating of the outer pore. *Neuron.* 32:635–648. https://doi.org/10.1016/s0896-6273(01)00503-7